Block of *HAC1* mRNA Translation by Long-Range Base Pairing Is Released by Cytoplasmic Splicing upon Induction of the Unfolded Protein Response

Ursula Rüegsegger,[2] Jess H. Leber,[2]
and Peter Walter[1]
Howard Hughes Medical Institute
Department of Biochemistry and Biophysics
University of California, San Francisco
San Francisco, California 94143

Summary

Expression of the yeast transcription factor Hac1p, which controls the unfolded protein response, is regulated posttranscriptionally. Hac1p is only produced when an intron at the 3′ end of its mRNA is removed by a nonconventional, regulated splicing reaction. We show that a previously unrecognized base-pairing interaction between the intron and the 5′ untranslated region is required and sufficient to block mRNA translation. Unspliced *HAC1* mRNA is stable, located in the cytosol, and is associated with polyribosomes, yet does not produce protein, indicating that the ribosomes engaged on the mRNA are stalled. We show that the polysomal, cytoplasmic pool of *HAC1* mRNA is a substrate for splicing, suggesting that the stalled ribosomes may resume translation after the intron is removed.

Introduction

In eukaryotic cells, secreted and membrane-bound proteins are folded and assembled in the endoplasmic reticulum (ER). The protein-folding capacity of the ER is adaptable: when the capacity of the ER is exceeded and, as a result, unfolded proteins accumulate in the ER, an intracellular signaling pathway, the unfolded protein response (UPR), is induced. The UPR leads to the increased synthesis of ER-resident proteins required for protein folding as well as many other components of the secretory pathway (Travers et al., 2000), thus enabling the cell to cope with the increased load of unfolded proteins in the ER (reviewed in Kaufman, 1999; Mori, 2000; Urano et al., 2000; Patil and Walter, 2001).

In yeast, the expression of UPR target genes is controlled by the UPR-specific transcription factor Hac1p (Cox and Walter, 1996; Kawahara et al., 1997). Hac1 protein is only detectable in cells when the UPR is induced, although its mRNA is present in uninduced and induced cells at comparable levels (Cox and Walter, 1996; Kawahara et al., 1997). The expression of Hac1p is therefore regulated posttranscriptionally. The key regulatory step to allow Hac1p synthesis upon UPR induction is the removal of an intron from *HAC1* mRNA by a nonconventional splicing mechanism. In this reaction, *HAC1* mRNA is cleaved at two splice sites by the transmembrane kinase/endonuclease Ire1p, and the thus liberated exons are then joined by tRNA ligase (Sidrauski

and Walter, 1997). This splicing event is induced by the activation of Ire1p, which responds to the accumulation of unfolded proteins in the ER lumen (Cox et al., 1993; Mori et al., 1993; Welihinda and Kaufman, 1996; Shamu and Walter, 1996; Bertolotti et al., 2000).

Both the spliced (*HAC1*[i]; "i" for *induced*) and the unspliced (*HAC1*[u]; "u" for *uninduced*) forms of *HAC1* mRNA encode proteins, called Hac1p[i] and Hac1p[u], respectively, which are identical except for their C-terminal tails. Splicing replaces a tail of 10 amino acids encoded in the intron of *HAC1*[u] mRNA with a tail of 18 amino acids encoded in the second exon of *HAC1*[i] mRNA. Only Hac1p[i], however, accumulates at detectable levels, while Hac1p[u] is apparently not expressed.

Several lines of evidence from previous studies suggest that the expression of Hac1p[u] is blocked at the translation level. In situ hybridization experiments localized *HAC1*[u] mRNA primarily in the cytoplasm (Chapman and Walter, 1997), thus ruling out that *HAC1*[u] mRNA is retained in the nucleus and can therefore not be translated. Also, a large portion of *HAC1*[u] mRNA comigrates with polyribosomes in sucrose gradients and can be immunoprecipitated with an antibody directed against an N-terminal epitope, demonstrating that the N terminus of the protein is made and exposed outside the ribosome (Cox and Walter, 1996; Chapman and Walter, 1997). These results suggest that translation of Hac1p[u] is initiated, but that ribosomes then stall on the mRNA before translation is completed. The alternative explanation that Hac1p[u] is synthesized but immediately degraded seems unlikely given that Hac1p[u] can be produced in yeast cells from intronless constructs and has a half-life similar to that of Hac1p[i] ($t_{1/2} \cong 2$ min; Kawahara et al., 1997; Chapman and Walter, 1997).

Here, we show that the *HAC1* mRNA intron represses translation of *HAC1*[u] mRNA in vivo and in vitro by base pairing with the *HAC1* 5′UTR. We find that the cytoplasmic pool of *HAC1*[u] mRNA is not a dead-end product but a substrate for the splicing reaction, indicating that splicing occurs in the cytoplasm on polyribosomes. The finding that *HAC1*[u] mRNA is polyribosome associated, yet no protein is synthesized, parallels findings for the developmentally regulated *lin-14* and *nanos* mRNAs from *Caenorhabditis elegans* and *Drosophila melanogaster*, respectively (Olsen and Ambros, 1999; Clark et al., 2000). Understanding the mechanism by which the translation of *HAC1* mRNA is controlled may therefore have implications for regulatory events beyond the unfolded protein response.

Results

Both the 5′UTR and Intron of Unspliced *HAC1*[u] mRNA Are Required for Translation Attenuation

Previous studies showed that the *HAC1*[u] mRNA intron represses expression of the green fluorescent protein (GFP) when placed in the 3′ untranslated region (UTR) of a GFP-encoding mRNA (Chapman and Walter, 1997).
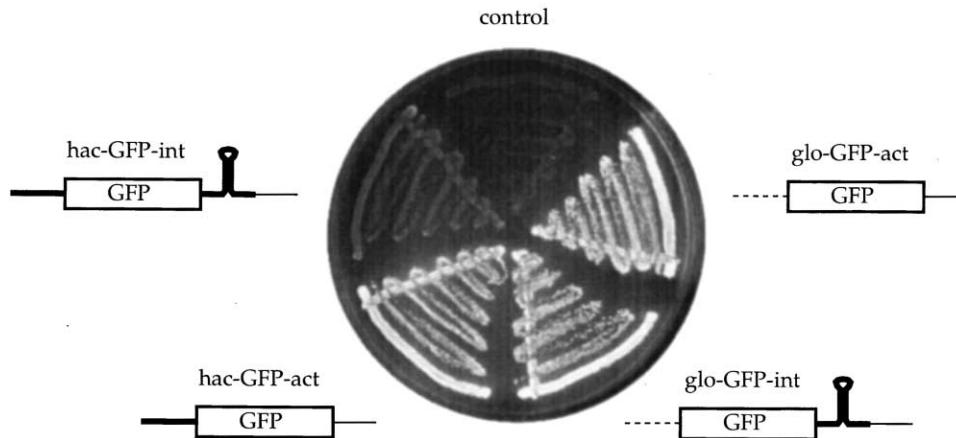
Figure 1. Translation Attenuation Requires both the *HAC1* 5'UTR and Intron

The yeast strain W303 transformed with the low-copy plasmid pRS315 carrying no insert (control), hac·GFP·int, hac·GFP·act, glo·GFP·int, or glo·GFP·act was plated on selective medium and the fluorescence of each strain determined by scanning the plate with a fluorescent scanner. Brightly fluorescent colonies appear white, nonfluorescent colonies black.

The constructs used in those studies contained not only the *HAC1* intron but also the *HAC1* promoter and the *HAC1* 5'UTR followed by a small portion of the Hac1p N terminus fused to GFP. To determine whether any elements in addition to the intron are necessary for translation attenuation, we expressed GFP (carrying no extra sequences) from a heterologous promoter with 5'UTR sequences derived either from *HAC1* or from *Xenopus* β-globin mRNA. For each 5'UTR, we made constructs that contained or lacked the *HAC1* intron. Our convention for naming constructs is as follows: the first three letters stand for the origin of the 5'UTR (i.e., "hac" for the *HAC1* 5'UTR and "glo" for the globin 5'UTR), the next three letters stand for the open reading frame (ORF) (i.e., "GFP" and "HAC" for Hac1p^u), and the last three letters for the sequences 3' of the ORF (i.e., "hac" for the *HAC1*^{u} 3'UTR, "int" for the *HAC1* intron followed by the *ACT1* 3'UTR, and "act" for the *ACT1* 3'UTR).

In agreement with previous results, cells showed only little fluorescence above background if they expressed GFP flanked by the *HAC1* 5'UTR and intron (Figure 1, compare hac·GFP·int with the empty-vector control). Surprisingly, replacement of the *HAC1* 5'UTR by the globin 5'UTR (glo·GFP·int) relieved translation attenuation of GFP to a similar degree as removal of the intron (hac·GFP·act), suggesting that both the *HAC1* 5'UTR and intron are required for translation attenuation. In both cases, cells were similarly fluorescent as cells expressing GFP flanked by the globin 5'UTR and the *ACT1* 3'UTR (glo·GFP·act).

To quantitate the effects of the *HAC1* 5'UTR and intron on GFP expression, we determined the mean fluorescence of the strains shown in Figure 1 by flow cytometry and measured the GFP mRNA levels by Northern blot (Table 1). From these data, we calculated the fluorescence of each strain relative to the amount of GFP mRNA and found that the intron repressed GFP expression 8-fold if the 5'UTR was from *HAC1* (compare the normalized fluorescence of hac·GFP·int with that of hac·GFP·act) but had only a minor effect if the 5'UTR was from

the heterologous globin mRNA (compare the normalized fluorescence of glo·GFP·int with that of glo·GFP·act). We therefore conclude that both the *HAC1* 5'UTR and intron are required for translation attenuation and that they act synergistically.

We next asked whether translation attenuation can be reconstituted in vitro in yeast translation extracts. We made four constructs similar to the GFP constructs described above but encoding HA-tagged Hac1p^u (HA-Hac1p^u). After in vitro transcription, we incubated equal amounts of capped mRNAs in nuclease-treated yeast in vitro translation extracts in the presence of [^{35}S]methionine and analyzed the products by SDS-polyacrylamide gel electrophoresis (SDS-PAGE) followed by autoradiography (Figure 2A). As equal amounts of mRNA were added to each reaction, the amount of HA-Hac1p^u synthesized is a measure of the translation efficiency of each construct.

HA-Hac1p^u has a predicted molecular mass of 27 kDa but migrates abnormally slowly on SDS-polyacrylamide gels (Kawahara et al., 1997). In addition to the primary translation product (Figure 2A, asterisk), multiple forms with higher molecular masses are expressed in vivo (Chapman and Walter, 1997) and in vitro (Figure 2A, lanes 2 to 5). The multiple bands are different forms of HA-Hac1p^u, since they are recognized by an antibody directed against the HA epitope (data not shown) and likely correspond to differently phosphorylated species of the primary translation product (Chapman and Walter, 1997).

We observed that hac·HAC·hac was translated only inefficiently in yeast in vitro translation extracts (Figure 2A, lane 2). Replacing the *HAC1*^{u} 3'UTR by the *ACT1* 3'UTR stimulated Hac1p^u synthesis 5-fold (Figure 2A, compare hac·HAC·hac with hac·HAC·act). This effect was robust: a 5- to 6-fold stimulation was observed over a wide range of mRNA concentrations and over the whole linear period of a time course experiment, and it was unaffected by heat denaturation followed by snap cooling of the mRNAs prior to addition to the extracts (data not shown). In vitro, translation from the globin

Table 1. Analysis of the Strains Shown in Figure 1 by Flow Cytometry

GFP construct [×]	mean fluorescence [$F_x/F_{hac\cdot GFP\cdot act}$]	GFP mRNA/SCR1 [$RNA_x/RNA_{hac\cdot GFP\cdot act}$]	normalized fluorescence [$(F_x/F_{hac\cdot GFP\cdot act})/(RNA_x/RNA_{hac\cdot GFP\cdot act})$]
hac·GFP·int	0.11 ± 0.01	0.91 ± 0.32	0.12 ± 0.04
hac·GRP·act	1.00 ± 0.06	1.00 ± 0.22	1.00 ± 0.23
glo·GFP·int	0.94 ± 0.08	0.68 ± 0.15	1.38 ± 0.33
glo·GFP·act	1.52 ± 0.08	0.88 ± 0.31	1.74 ± 0.62

The strains from Figure 1 were grown in selective liquid medium and their mean fluorescence F_x (x stands for hac·GFP·int, hac·GFP·act, glo·GFP·int, or glo·GFP·act) was determined by flow cytometry. The amounts of mRNA encoding GFP relative to the amounts of *SCR1* RNA [RNA_x] were determined for the same cultures by Northern blot analysis and used to normalize the fluorescence of each strain. The results shown are the averages of at least three independent experiments.

5′UTR was 2-fold less efficient than translation from the *HAC1* 5′UTR (Figure 2A, compare glo·HAC·act with hac·HAC·act), but translation from this heterologous 5′UTR was unaffected by the *HAC1*^u 3′UTR (Figure 2A, compare glo·HAC·act with glo·HAC·hac). While, in vitro, small amounts of Hac1p^u are still expressed from the hac·HAC·hac constructs, no Hac1p^u is detected in vivo in the absence of UPR induction. The reason for this apparently reduced efficiency of translation attenuation in vitro is unknown, but perhaps could be due to limiting amounts of a factor necessary to promote inhibition.

Taken together, these results show that *HAC1*^u mRNA is translationally attenuated in vitro and that attenuation requires sequences both 5′ and 3′ of the Hac1p^u ORF. The *cis*-acting elements at the 3′ end are likely to be located in the *HAC1* intron, since the intron repressed GFP expression in the context of a heterologous 3′UTR (Figure 1 and Table 1).

A Direct Interaction of the *HAC1* 5′UTR and Intron Attenuates *HAC1*^u mRNA Translation In Vitro

The observation that the *HAC1* 5′UTR and intron act synergistically to attenuate translation suggested that they interact, either directly or indirectly. Such an interaction of regions at distant sites of the mRNA may be mediated by base pairing, by RNA binding proteins, or both. Indeed, inspection of the intron for sequences complementary to the *HAC1* 5′UTR revealed a G-rich stretch of 19 nucleotides (nt), 16 of which could potentially base pair with the 5′UTR (Figure 2B).

We therefore asked next whether translation attenuation by the *HAC1* 5′UTR and intron is mediated by the base pairing proposed in Figure 2B. If this base pairing is required for translation attenuation, disrupting the 5′UTR-intron interaction by annealing an oligonucleotide to the sequences predicted to be involved should relieve translation attenuation of *HAC1*^u mRNA. To test this prediction, 10- and 100-fold molar excesses of 2′-O-methyl oligoribonucleotides were preannealed to hac·HAC·hac or hac·HAC·act mRNAs, which were then added to translation extracts (Figure 2C). Since it was shown previously that oligonucleotide-mRNA hybrids located within the 5′UTR, but not the 3′UTR, inhibit translation in vitro (Johansson et al., 1994), we first looked at the effect of an oligonucleotide complementary to the intron sequences shown in Figure 2B (anti-intron). This oligonucleotide stimulated translation of hac·HAC·hac such that it was now as efficiently translated as hac·HAC·act (Figure 2C, compare lane 6 with

lane 9 or 13) but had no effect on the translation of hac·HAC·act (Figure 2C, compare lanes 12 and 13 with lane 9). As expected, a nonspecific oligonucleotide, which carried sequences from the *HAC1* ORF (sense-ORF), had no effect on translation of hac·HAC·hac (Figure 2C, compare lanes 3 and 4 with lane 2) or hac·HAC·act (Figure 2C, compare lanes 10 and 11 with lane 9). These results show that the intron sequences targeted by the antiintron oligonucleotide are necessary for the attenuation of *HAC1*^u mRNA translation.

As predicted from previous experiments (Johansson et al., 1994), an oligonucleotide complementary to the *HAC1* 5′UTR and targeted to the same site as the intron (anti-5′UTR) inhibited translation of both constructs (Figure 2C, lanes 7, 8, 14, and 15). The inhibition caused by the anti-5′UTR oligonucleotide was virtually complete, whereas the *HAC1* intron, when present in *cis* in the mRNA, attenuated translation only 5- to 6-fold (Figure 2C, compare lane 2 with lane 9). The stronger inhibitory effect of the oligonucleotide is perhaps due to the fact that an oligonucleotide is more flexible than the corresponding stretch of nucleotides as part of a long RNA, in which structural and topological constraints may hinder complete base pairing over an extended region. For *HAC1* mRNA, incomplete base pairing may be essential to allow the dissociation of the intron and 5′UTR after excision of the intron from the RNA upon splicing.

Disruption of the Interaction between the *HAC1* 5′UTR and Intron Leads to the Accumulation of Hac1p^u In Vivo

If the intron sequences targeted by the antiintron oligonucleotide are required for translation attenuation of *HAC1*^u mRNA in vivo, then mutating those nucleotides should relieve translation attenuation and lead to the accumulation of Hac1p^u. Furthermore, if the intron sequences inhibit translation by interacting with the 5′UTR, then introducing mutations in the 5′UTR compensatory to the mutations in the intron should restore repression. To test these predictions, we generated three mutant forms of HA-*HAC1* mRNA (Figure 3A). To mutate the intron, we replaced the intron sequences with sequences from the 5′UTR (pJL179). To restore base pairing in the intron mutant, we introduced compensatory mutations in the 5′UTR by replacing the 5′UTR sequences with sequences from the intron (pJL177). We also constructed a mutant in which only the 5′UTR was mutated (pJL178). This mutant is predicted to behave
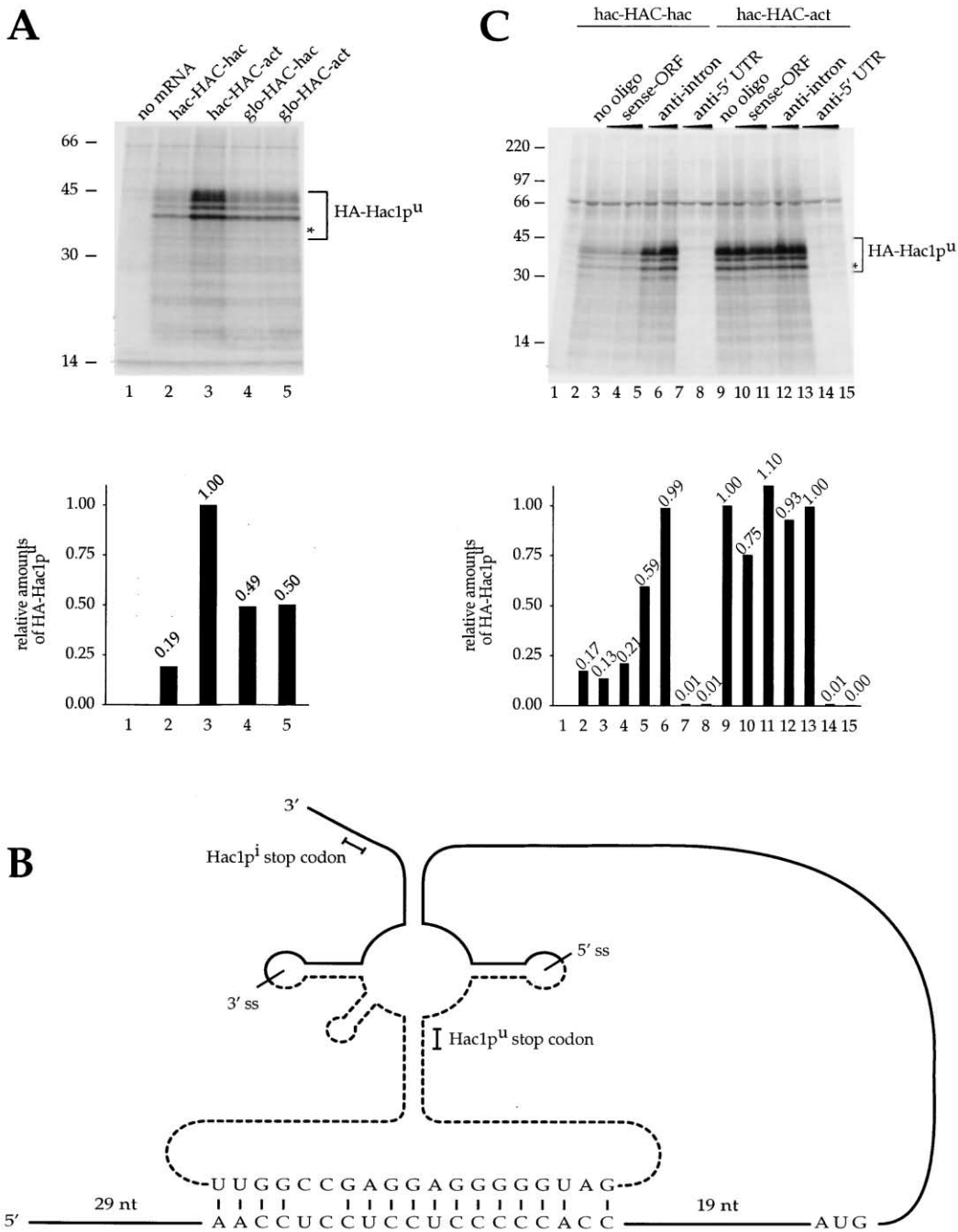
Figure 2. In Vitro Reconstitution of Translation Attenuation by the *HAC1* 5′UTR and Intron

(A) The transcripts indicated at the top were incubated in yeast extract in the presence of [³⁵S]methionine for 50 min and the products analyzed by SDS-PAGE followed by autoradiography. The molecular masses of the size standards are indicated in kDa on the left. The asterisk on the right marks the primary translation product while the bracket indicates all forms of HA-Hac1pᵘ. The amount of HA-Hac1pᵘ synthesized from each template relative to the amount synthesized from hac·HAC·act is shown below each lane.

(B) The *HAC1* 5′UTR and intron contain complementary sequences. Exonic sequences are shown as solid lines, intronic sequences as dashed lines. The secondary structure shown is based on predictions but the splice sites have been shown experimentally to be located in the loops of stem-loop structures (Gonzalez et al., 1999). The model is not drawn to scale. ss: splice site.

(C) An oligonucleotide directed against the intron stimulates translation of *HAC1ᵘ* in vitro. The transcripts hac·HAC·hac (lanes 2–8) and hac·HAC·act (lanes 9–15) annealed to the oligonucleotides indicated at the top were incubated in yeast extract in the presence of [³⁵S]methionine for 50 min and the products analyzed by SDS-PAGE followed by autoradiography. The molecular masses of the size standards are indicated in kDa on the left. The asterisk on the right marks the primary translation product while the bracket indicates all forms of HA-Hac1pᵘ. The amount of HA-Hac1pᵘ synthesized under each condition relative to the amount synthesized from hac·HAC·act in the absence of any oligonucleotide is shown at the bottom. Lane 1: no mRNA; lanes 2 and 9: no oligonucleotide; lanes 3, 5, 7, 10, 12, and 14: 2 pmol of the oligonucleotide indicated at the top; lanes 4, 6, 8, 11, 13, and 15: 20 pmol of the oligonucleotide indicated at the top.

A

plasmid	description and sequences of relevant parts of 5'UTR and intron
pJC316	intron wild-type: 3' U U G G C C G A G G A G G G G U 5' 5'UTR wild-type: 5' A A C C U C C U C C U C C C C A 3'
pJL179	intron mutated: 3' A A C C U C C U C C U C C C C A 5' 5'UTR wild-type: 5' A A C C U C C U C C U C C C C A 3'
pJL178	intron wild-type: 3' U U G G C C G A G G A G G G G U 5' 5'UTR mutated: 5' U U G G C C G A G G A G G G G U 3'
pJL177	intron mutated: 3' A A C C U C C U C C U C C C C A 5' 5'UTR mutated: 5' U U G G C C G A G G A G G G G U 3'

B

pJC316 (wt) pJL179 (intron mt) pJL178 (5'UTR mt) pJL177 (bp rest.)

– HA-HAC1^u
– HA-HAC1^i
*
**
– SCR1

1 2 3 4 5 6 7 8

82   38   59   84   % splicing

C

pJC316 (wt), pJL179 (intron mt), pJL178 (5' UTR mt), pJL177 (bp rest.), pJC834 (11A-Hac1p^u), pJC316 (wt), pJL179 (intron mt), pJL178 (5' UTR mt), pJL177 (bp rest.)

– – – – + + + + + DTT

] HA-Hac1p

longer exposure:

] HA-Hac1p

1 2 3 4 5 6 7 8 9

HA-Hac1p^u [ ] ←HA-Hac1p^i

2 5 6 7

D

pJL179 (intron mt)   pJC316 (wt)

DTT   –   +

protein loaded: 8x   1x   2x

HA-Hac1p^u [ ]   ←HA-Hac1p^i

1   2   3

Figure 3. Disruption of the Interaction between the *HAC1* 5′UTR and Intron Leads to the Accumulation of Hac1p^u and Inhibits Splicing

A Δ*hac1* yeast strain was transformed with plasmids pJC316, pJL179, pJL178, pJL177, or pJC834 (a previously described plasmid from which HA-Hac1p^u is expressed constitutively [Chapman and Walter, 1997]) and grown in selective liquid medium. The UPR was induced by adding 8 mM DTT for 50 min.

(A) Overview of the relevant sequences in plasmids pJC316, pJL179, pJL178, and pJL177. Wild-type sequences are shown in bold.

(B) Northern blot analysis. Fifteen micrograms total RNA was separated on a 1.5% w/v agarose gel and transferred to a membrane, which was incubated with probes directed against the *HAC1* 5′ exon and *SCR1*. The amount of *HAC1* splicing after UPR induction is indicated at the bottom for each plasmid. The positions of HA-*HAC1^u*, HA-*HAC1^i*, and *SCR1* are indicated on the right. The asterisks on the right indicate potential splicing intermediates (one asterisk: 5′ exon-intron; two asterisks: 5′ exon). wt: wild-type; mt: mutant; bp rest.: base pairing restored.

(C) Western blot analysis. Twenty-five micrograms of protein were separated on a 12.5% w/v SDS-polyacrylamide gel and transferred to a nitrocellulose membrane. HA-Hac1p was detected with an antibody directed against the HA tag and the ECL system. The middle panel is a longer exposure of the blot shown in the top panel. The brackets on the right of the top two panels indicate the different forms of HA-Hac1p. The open arrowhead on the left indicates a band unrelated to HA-Hac1p visible upon longer exposure, which is also detectable in extracts of the Δ*hac1* strain transformed with an empty plasmid (data not shown). Lanes 2 (long exposure), 5, 6, and 7 (short exposure) are shown 2-fold enlarged at the bottom and the positions of the multiple forms of HA-Hac1p^u and HA-Hac1p^i are indicated for each lane by brackets and diamonds, respectively.

(D) Titration of selected samples from (C). Twenty-five micrograms (lane 1), three micrograms (lane 2), and six micrograms (lane 3) protein were separated in parallel on 12.5% w/v SDS-polyacrylamide gels and transferred to nitrocellulose membranes. HA-Hac1p was detected with an antibody directed against the HA tag and the ECL Plus system. The amount of total protein loaded relative to the amount loaded in lane 2 is indicated above each lane.

as the intron mutant except that the two mutants differ in the sequences of their 5′UTRs and may therefore differ in the efficiency with which they are translated.

We introduced the three mutants or, as a control, wild-type HA-*HAC1* (pJC316 [Cox and Walter, 1996]) on plasmids into a Δ*hac1* strain and asked first whether the mutant and wild-type mRNAs were expressed at comparable levels and whether the mutations affected splicing upon UPR induction. Northern blot analysis revealed that the amounts of HA-*HAC1* mRNA in uninduced cells were 2- to 4-fold lower in the strains with disrupted base pairing than in the strains with intact base pairing (Figure 3B, compare lanes 1 and 7 with lanes 3 and 5). Upon UPR induction, HA-*HAC1* mRNA levels increased in all strains between 1.4- and 3.5-fold (for example, compare lanes 3 and 4). Whether these effects were due to transcriptional regulation, to differences in mRNA stability, or to a combination of the two remains to be investigated.

Splicing efficiency of the forms of HA-*HAC1* mRNA with intact 5′UTR-intron base pairing was above 80% (Figure 3B, lanes 2 and 8). In contrast, splicing efficiency in the mutants with disrupted base pairing was reduced to ∼40% and ∼60%, respectively (Figure 3B, lanes 4

and 6). Thus, the 5′UTR-intron interaction is necessary for efficient *HAC1* mRNA splicing.

We next monitored the expression of HA-Hac1p in uninduced and UPR-induced cells by Western blot with an antibody directed against the HA tag (Figure 3C). As expected, no protein was synthesized at detectable levels from the wild-type plasmid in uninduced cells (pJC316; Figure 3C, top and middle panel, lane 1; the band indicated with an open arrowhead is unrelated to HA-Hac1p). Removal of the intron by splicing after induction of the UPR with dithiothreitol (DTT) led to the synthesis of HA-Hac1p^i (Figure 3C, lane 6, marked with a diamond in the bottom panel).

Intriguingly, when the base pairing was disrupted by mutations in either the intron (pJL179) or the 5′UTR (pJL178), HA-Hac1p^u accumulated in uninduced cells (Figure 3C, middle panel, lanes 2 and 3). The multiple forms of HA-Hac1p^u (indicated by brackets and shown enlarged in the bottom panel of Figure 3C) comigrated by SDS-PAGE with HA-Hac1p^u expressed constitutively from an intronless construct described previously (pJC834 [Chapman and Walter, 1997]; Figure 3C, bottom panel, lane 5). Less protein was synthesized from the 5′UTR mutant, indicating that translation from this 5′UTR is less efficient than from the wild-type 5′UTR. Importantly, no Hac1p was synthesized in uninduced cells if the base pairing was restored by compensatory mutations in both the intron and the 5′UTR (pJL177; Figure 3C, top and middle panel, lane 4). For this construct, induction of the UPR resulted in synthesis of HA-Hac1p^i (Figure 3C, lane 9), thus recapitulating the wild-type situation. Both mutants in which the base pairing between the 5′UTR and intron was disrupted expressed a mixture of HA-Hac1p^u and HA-Hac1p^i upon UPR induction (Figure 3C, lanes 7 and 8; compare lane 7 with lanes 5 and 6 in the enlargement), which is not surprising given that these cells contained comparable amounts of HA-*HAC1*^{u} and HA-*HAC1*^{i} mRNA and that the mutant forms of HA-*HAC1*^{u} mRNA were efficiently translated in uninduced cells.

For all strains, the differences in protein levels correlated with the differences in mRNA levels as confirmed by quantitation of Western blots (data not shown), if mRNAs with identical 5′UTR sequences were compared. Most importantly, our data show that if the base pairing interaction was disrupted by mutating the intron, the mutant *HAC1*^{u} mRNA was translated in uninduced cells with an efficiency comparable to that of wild-type *HAC1*^{i} mRNA produced by splicing: the level of Hac1p^u in mutant uninduced cells was 5-fold lower than that of Hac1p^i in wild-type UPR-induced cells as determined by quantitative Western blot analysis with a radio-iodinated secondary antibody (data not shown), and the mRNA level in mutant cells was 6-fold lower than that in wild-type cells (Figure 3B, compare lane 3 with lane 2). Qualitatively, these conclusions are confirmed by the Western blot analysis shown in Figure 3D: to give an approximately equal ECL signal intensity, we needed to load 4- to 8-fold more total protein per gel lane from the mutant than from the wild-type strain (compare lane 1 with lanes 2 and 3).

Thus, taken together, the data presented so far argue that the *HAC1* 5′UTR interacts with the *HAC1* intron by base pairing and that this interaction is the primary, if not only, determinant of *HAC1*^{u} mRNA translation attenuation.

Base Pairing of the *HAC1* 5′UTR and Intron Diminishes the Loading of Ribosomes onto *HAC1*^{u} mRNA

To a first approximation, the efficiency of translation of an mRNA correlates with the number of ribosomes that are engaged with it. To determine the degree to which ribosome association of *HAC1*^{u} mRNA changes when the *HAC1* 5′UTR-intron interaction is disrupted, we fractionated polyribosomes from the wild-type and mutant strains described in Figure 3 by sedimentation in sucrose gradients. We isolated total RNA from all fractions across the gradients and analyzed it by Northern blot (Figure 4A). Wild-type *HAC1*^{u} mRNA fractionated into two pools: about half (42%) of *HAC1*^{u} mRNA was recovered from the top of the gradient and therefore was not ribosome associated (pJC316; fractions 1 to 4 in Figure 4A; quantitation in Figure 4B). The remainder (58%) was recovered from heavier fractions indicating occupancies ranging from one to ten or more ribosomes per mRNA (pJC316; fractions 5 to 14 in Figures 4A and 4B). In contrast, if the intron was mutated so that it could no longer base pair with the 5′UTR, only a small amount (9%) of *HAC1*^{u} mRNA was recovered from the top of the gradient, whereas the majority of the mRNA (91%) was ribosome associated (pJL179; fractions 5 to 14 in Figures 4A and 4B). A similar distribution over the gradient was found for the 5′UTR mutant (pJL178; Figure 4B). Restoring the base pairing by mutating both the *HAC1* 5′UTR and intron reestablished the degree of ribosome association found for the wild-type construct (compare pJL177 with pJC316 in Figure 4B). These data suggest that the base pairing of the *HAC1* 5′UTR and intron diminishes ribosome loading onto *HAC1*^{u} mRNA.

Moreover, the data also underscore a previously raised paradox: if 58% of wild-type *HAC1*^{u} mRNA was indeed translated as the polyribosome profile in Figure 4A suggests, and if translation occurred at the same rate as translation of the mutants with disrupted base pairing, then Hac1p^u should accumulate in wild-type cells at detectable levels, which is not what we observe. We estimate that, if *HAC1*^{u} mRNA was translated at even 10% of the rate of the base-pair-disrupted mutant mRNA, Hac1p^u would have been readily detectable by Western blot analysis.

To provide independent evidence that the portion of *HAC1*^{u} mRNA sedimenting as high-molecular-mass complexes is indeed ribosome associated, we determined whether *HAC1*^{u} mRNA coprofiles with the UV absorbance reflective of the position of mRNAs associated with one ribosome, two ribosomes, etc. To this end, we collected many small fractions from the middle of a gradient and determined the presence of *HAC1*^{u} mRNA by Northern blot analysis. As shown in Figure 4C, the distribution of *HAC1*^{u} mRNA is discontinuous, with peaks and valleys precisely following the position of ribosomes.

Taken together, the data show that *HAC1*^{u} mRNA is associated with ribosomes that are not actively translating.
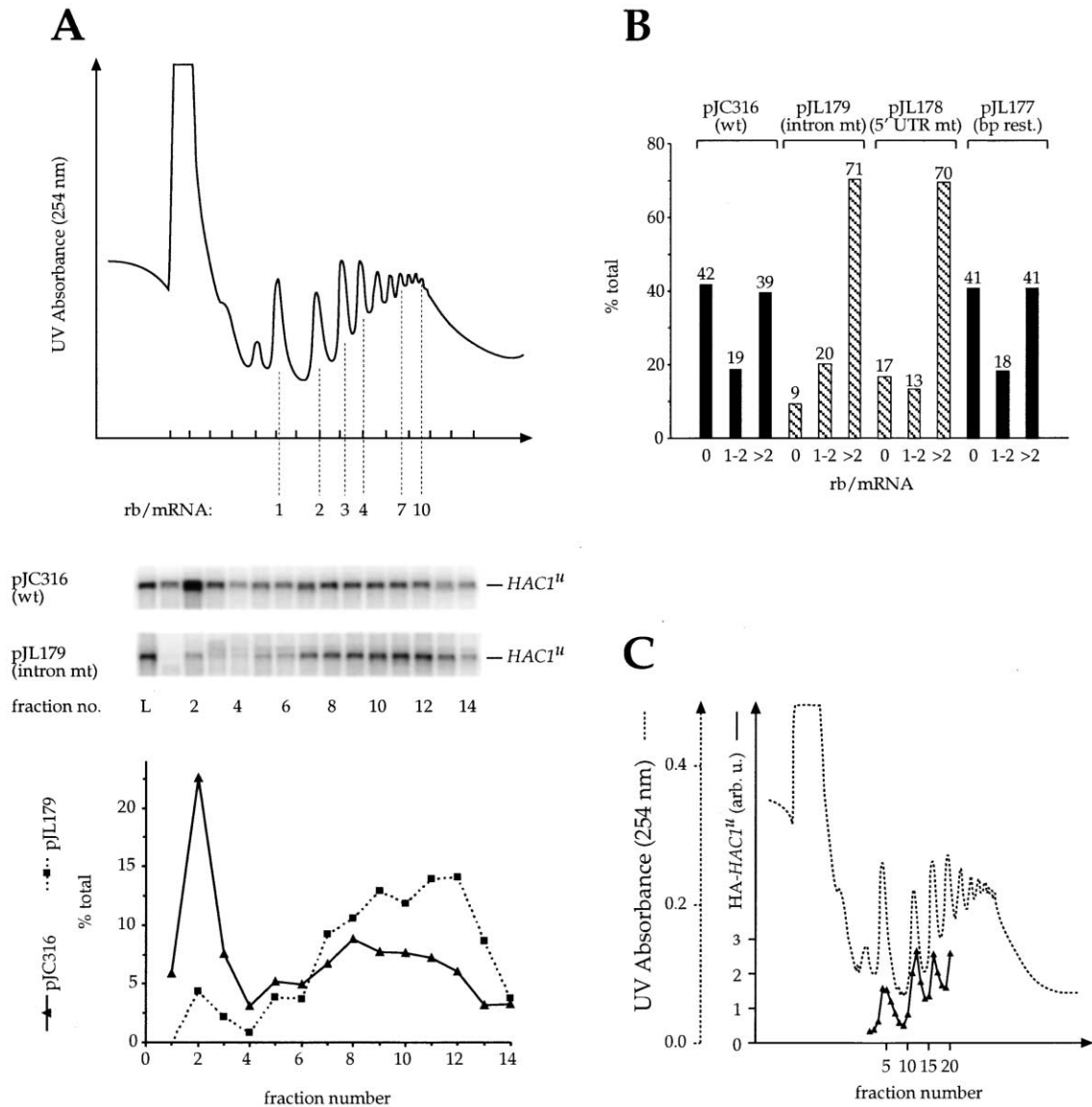
Figure 4. The Interaction of the *HAC1* 5′UTR and Intron Diminishes the Loading of Ribosomes onto *HAC1ᵘ* mRNA

(A) Extracts from Δ*hac1* strains carrying either pJC316 or pJL179 were fractionated over 10%–50% w/v sucrose gradients and 750 μl fractions were collected across the gradients. The direction of sedimentation is from left to right. UV absorbance profile at 254 nm (top), Northern blot analysis (middle), and quantitation of the Northern blots (bottom). Northern blots: 50% of the fractions indicated at the bottom and 5% of the loads (L) were separated on 1.5% w/v agarose gels and the RNA transferred to membranes, which were incubated with a probe directed against the *HAC1* 5′ exon and intron. Note that the HA-*HAC1* mRNA levels are substantially lower in the strain carrying pJL179 than in the one carrying pJC316, but the images of the two Northern blots were processed to give similar signal intensities. The strain analyzed is indicated at the left and the number of ribosomes (rb) per mRNA between the profile and the Northern blots. wt: wild-type; mt: mutant. Quantitation: the amount of HA-*HAC1* mRNA in each fraction is expressed as percentage of the total amount of HA-*HAC1* mRNA recovered over the gradient (% total).

(B) Extracts from Δ*hac1* strains carrying either pJC316, pJL179, pJL178, or pJL177 were fractionated over 10%–50% w/v sucrose gradients, fractions collected and analyzed by Northern blot as described in (A), and the number of ribosomes per mRNA was determined for each fraction based on the UV absorbance profile. The amounts of HA-*HAC1* mRNA associated with 0, 1–2, and more than 2 ribosomes are shown as percentage of the total amount of HA-*HAC1* mRNA recovered over the gradient (% total). The analysis across the gradient is shown in detail in (A) for pJC316 and pJL179.

(C) Extract from the Δ*hac1* strain carrying pJC316 was fractionated over a 10%–50% w/v sucrose gradient and twenty 180 μl fractions were collected from the middle of the gradient. The direction of sedimentation is from left to right. The UV absorbance profile at 254 nm is shown with a stippled line and the quantitation of HA-*HAC1ᵘ* mRNA by Northern blot with a solid line. Northern blot analysis was carried out as described in (A). arb. u.: arbitrary unit of quantitation by phosphor screen autoradiography.

The Cytoplasmic Pool of *HAC1ᵘ* mRNA Is a Substrate for Splicing

The peculiar disposition of the unspliced *HAC1ᵘ* mRNA on stalled, cytoplasmic polyribosomes raises the question of whether these polyribosomes have a physiological role in the cell. On one hand, *HAC1ᵘ* polyribosomes could be dead-end products that are permanently arrested and eventually decay; all spliced *HAC1ⁱ* mRNA

would thus result from newly transcribed *HAC1ᵘ* mRNA. On the other hand, we can envision positive functions for the cytoplasmic polysomal pool of *HAC1ᵘ* mRNA. For example, *HAC1ᵘ* mRNA might be translated to produce Hac1pᵘ in response to some unknown physiological stimulus that leads to disruption of the base pairing of the 5′UTR and intron, thus allowing translation. An alternative and not mutually exclusive possible function for the cytoplasmic pool of *HAC1ᵘ* mRNA is that it is the precursor of spliced *HAC1ⁱ* mRNA.

To address this latter scenario experimentally, we determined whether *HAC1ᵘ* mRNA could be spliced after transcription was inhibited. To this end, we took advantage of a temperature-sensitive allele of the largest subunit of RNA polymerase II (*rpb1-1*), which allowed us to shut off transcription by shifting the cells to the nonpermissive temperature of 37°C (Nonet et al., 1987). In the experiment shown in Figure 5A, we induced the UPR by the addition of DTT 10, 20, and 40 min after a shift to 37°C and followed the effect of the DTT treatment on *HAC1* mRNA by Northern blot in a time course experiment. *HAC1ᵘ* mRNA decayed with a $t_{1/2}$ of ~25 min while, as expected, the levels of the RNA polymerase III transcript *SCR1* RNA remained unchanged (data not shown). Upon addition of DTT, *HAC1ᵘ* mRNA was efficiently spliced (50%–65% splicing within 5 min). Most importantly, splicing efficiency did not diminish appreciably when the UPR was induced as much as 40 min after the transcriptional block. Thus, splicing was still efficient even after almost two half-lives of the mRNA had passed and any transient nuclear pool of freshly transcribed mRNA should have been depleted by export to the cytoplasm. Given that in situ hybridization experiments showed that *HAC1ᵘ* mRNA is primarily localized in the cytoplasm (Chapman and Walter, 1997), the efficient splicing of *HAC1* mRNA in the absence of de novo transcription suggests that *HAC1ⁱ* mRNA is produced by splicing of the cytoplasmic pool of *HAC1ᵘ* mRNA.

To test whether polyribosome-associated *HAC1* mRNA can be a substrate for cleavage and ligation in vivo, we froze translating ribosomes on their respective mRNAs with the elongation inhibitor cycloheximide, thus preventing the running-off as well as the loading of ribosomes onto the mRNA, and then added DTT to induce the UPR. After UPR induction in the presence of cycloheximide, any spliced *HAC1* mRNA that is associated with polyribosomes must have been polyribosome-associated prior to and during the splicing reaction. We found, however, that after cycloheximide pretreatment, cells were completely refractory to UPR induction by DTT (data not shown). We reasoned that, as a consequence of inhibition of protein synthesis by cycloheximide, the ER may be depleted of proteins since no proteins are imported into the ER but export into the secretory pathway continues. Addition of the reducing agent DTT would therefore fail to induce the UPR after cycloheximide pretreatment. To alleviate this problem, we took advantage of a temperature-sensitive allele of *SEC12*, which is required for vesicle transport from the ER to the Golgi (Oka et al., 1991; Novick et al., 1980). When the *sec12-1* cells were first shifted to the nonpermissive temperature, at which protein export from the ER into the secretory pathway is blocked, and then treated with cycloheximide to freeze ribosomes on
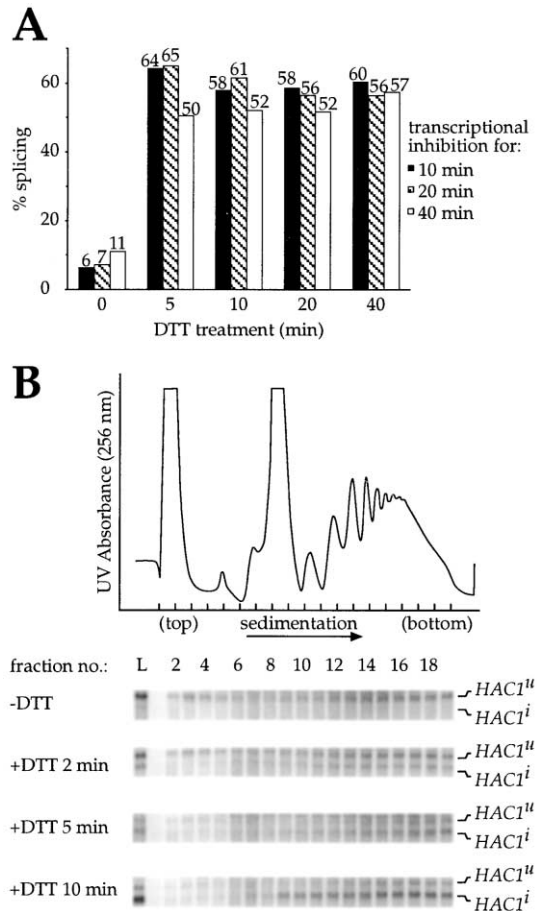
Figure 5. The Cytoplasmic Pool of *HAC1ᵘ* mRNA Is a Substrate for Splicing

(A) Yeast cells expressing a temperature-sensitive allele of the largest subunit of RNA polymerase II were shifted to the nonpermissive temperature for 10, 20, and 40 min. At these time points, DTT was added to a final concentration of 8 mM. Total RNA was isolated from aliquots taken immediately before and 5, 10, 20, and 40 min after the addition of DTT. The amount of *HAC1* mRNA splicing was determined for each time point by Northern blot analysis with a probe directed against the 5′ exon.

(B) Yeast cells expressing a temperature-sensitive allele of *SEC12*, required for vesicle transport from the ER to Golgi, were shifted to the nonpermissive temperature for 2 min, and then cycloheximide was added to a final concentration of 60 μg/ml. DTT was added after 1 min to a final concentration of 8 mM, and extracts were prepared from aliquots taken immediately before and 2, 5, and 10 min after the addition of DTT. Extracts were fractionated over a 10%–50% sucrose gradient and analyzed by Northern blots, as in Figure 4C.

mRNAs, subsequent addition of DTT was now able to induce the UPR.

We therefore used this extended experimental protocol to assess whether polyribosome-associated *HAC1* mRNA is a substrate for the splicing reaction. To this end, we induced the UPR with DTT *sec12-1* cells that were first shifted to 37°C for 2 min and then cycloheximide-treated to freeze polyribosomes (Figure 5B). We then fractionated, on sucrose gradients, cell extracts prepared at different times after DTT addition and analyzed fractions by Northern blot. As expected, in the

absence of DTT, polyribosome-associated *HAC1* is unspliced ("*HAC1*^u", Figure 5B, top). In contrast, as a function of time after DTT addition, increasing amounts of spliced *HAC1*ⁱ mRNA were produced (Figure 5B, lower panels). Importantly, virtually all spliced *HAC1*ⁱ mRNA produced in the presence of cycloheximide was polyribosome associated, thus supporting the notion that cytoplasmic, polyribosome assciated *HAC1*^u mRNA can be spliced.

Discussion

We have demonstrated both in vitro and in vivo that a long-range base pairing interaction between the *HAC1* mRNA intron and 5'UTR is required for attenuation of translation of unspliced *HAC1*^u mRNA. In particular, we have shown that upon disruption of the interaction by mutation, Hac1p^u is synthesized from the unspliced mRNA with approximately the same efficiency as Hac1pⁱ from the spliced mRNA. Thus, base pairing between the *HAC1* mRNA intron and 5'UTR is key to preventing Hac1p from being synthesized unless the intron is removed by splicing upon accumulation of unfolded proteins in the ER. In agreement with previous studies, we found a large portion of the cellular *HAC1*^u mRNA engaged in polyribosomes, which, we propose, must be translationally arrested, as no Hac1p^u can be detected in these cells. Moreover, we show that splicing does not require de novo transcription and that polyribosome-associated *HAC1*^u mRNA is a substrate for splicing in vivo. Taken together with the observation that the cellular pool of *HAC1*^u mRNA has been localized to the cytoplasm by in situ hybridization experiments (Chapman and Walter, 1997), these results suggest that *HAC1*^u mRNA splicing is a cytoplasmic event.

Inhibition of translation by the interaction of the 5' and 3'UTRs of an mRNA may be a generally applicable principle. Several natural and artificial cases have been described for yeast, plant, and animal cells (Spena et al., 1985; Kozak, 1989; van den Heuvel et al., 1990; Vega Laso et al., 1993). Moreover, considering the 5'UTR as an antisense RNA targeted against the intron to repress translation points to a striking parallel between translation attenuation of *HAC1*^u mRNA and the developmental regulation of *lin-14* expression in *Caenorhabditis elegans*: the small, noncoding *lin-4* RNA represses the expression of *lin-14* posttranscriptionally by base pairing with its 3'UTR (Lee et al., 1993; Wightman et al., 1993). As is the case for *HAC1*^u mRNA, the repressed *lin-14* mRNA is polyribosome associated, and part of *lin-4* RNA cosediments with polyribosomes (Olsen and Ambros, 1999). Stalling ribosomes by an antisense mechanism involving the 3'UTR may therefore be a more general way to inhibit translation.

The accumulation of *HAC1*^u mRNA on polyribosomes is puzzling, however, in light of the fact that the proposed translational regulation through the long-range base-pairing interaction involves the 5'UTR: as small ribosomal subunits have to traverse the 5'UTR to reach the start codon, one would expect a base-pairing interaction involving the 5'UTR to inhibit ribosome loading. Strong secondary structure elements or proteins bound to the 5'UTR are known to inhibit initiation of other mRNAs
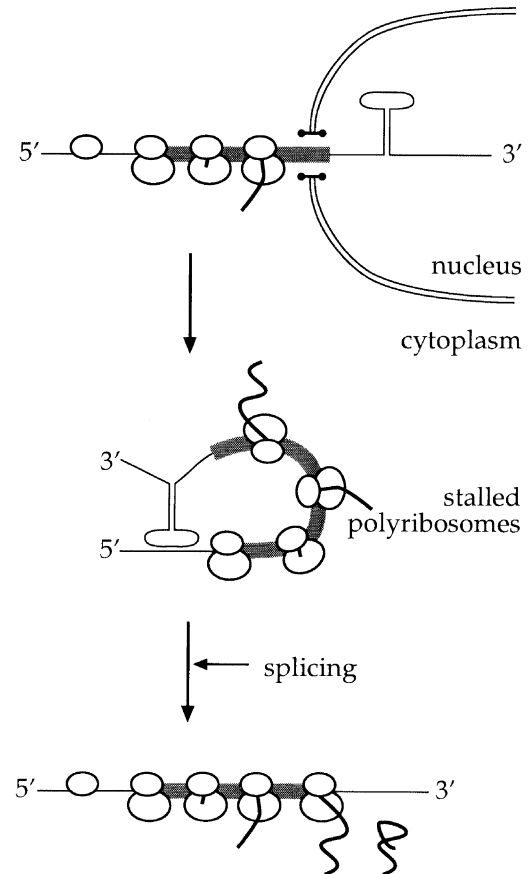
Figure 6. A Model for Translation Attenuation and Its Relief by Cytoplasmic Splicing

(reviewed in Gray and Wickens, 1998). Indeed, when we compared intron-containing and intronless versions of *HAC1*^u mRNA in in vitro translation reactions, translation was impaired at the initiation step (data not shown). How then could one explain that a large portion of *HAC1*^u mRNA becomes engaged in polyribosomes in vivo?

One possible scenario is that those ribosomes are loaded onto *HAC1*^u mRNA before the base pairing is established (Figure 6). In higher eukaryotes, mRNAs are exported from the nucleus 5' end first, and ribosomes engage with the leading ends of the mRNAs as soon as they reach the cytoplasm (Mehlin et al., 1992). Ribosomes may thus start immediately translating *HAC1*^u mRNA during the export of the mRNA from the nucleus to the cytoplasm, while the 3' end of the message is still in the nucleoplasm. Only after the 3'UTR of *HAC1*^u mRNA is exported to the cytosol can the intron interact with the 5'UTR. As the long-range base-pairing interaction is formed, it might not only inhibit the loading of new ribosomes but also stall and trap those ribosomes that are already engaged on the mRNA, possibly through inducing the formation of tight secondary and tertiary structural elements that the ribosomes cannot traverse.

The notion that the high-molecular-mass complexes with which *HAC1*^u mRNA is associated are indeed polyribosomes is strongly supported by the coprofiling experiment shown in Figure 4C. Moreover, as has been shown previously, a large portion of HA-*HAC1*^u mRNA

can be immunoprecipitated with antibodies directed against the HA epitope, indicating that each of these mRNAs contains at least one functionally engaged ribosome displaying the N terminus of HA-Hac1p^u (Chapman and Walter, 1997). However, in addition to the polyribosome-associated pool, we also isolated *HAC1*^{u} mRNA in a ribosome-free form (Figure 4A). What is the origin of the two *HAC1*^{u} mRNA pools?

Since no significant nuclear pool of *HAC1*^{u} mRNA was detected by in situ hybridization (Chapman and Walter, 1997), both the ribosome-free and the polyribosome-associated pool of *HAC1*^{u} mRNA are likely to reside in the cytoplasm. With this premise, two scenarios could account for the heterogeneous distribution of *HAC1*^{u} mRNA in sucrose gradients. First, upon nuclear export, some *HAC1*^{u} mRNA molecules may escape ribosome loading. The distribution between the ribosome-free and the polyribosome-associated pool would then depend on the ratio of the nuclear export and the translation initiation rates. Alternatively, upon nuclear export, all *HAC1*^{u} mRNAs may become polyribosome associated at first, but the stalled ribosomes eventually fall off, either in vivo or upon cell fractionation, thus generating the two pools.

Mutant *HAC1*^{u} mRNAs from which the translation block was removed by disrupting the 5′UTR-intron interaction also showed a splicing defect (Figure 3B). The 5′UTR-intron interaction is therefore not only essential to repress Hac1p expression in uninduced cells but also to allow efficient splicing and Hac1p synthesis upon UPR induction. Base pairing may thus provide an additional *cis*-acting element for *HAC1* mRNA splicing, which is not essential but stimulatory. According to this view, the 5′UTR-intron interaction might be required to correctly position the splice sites in the stem-loop structures which have been shown to be essential for splicing in vitro (Gonzalez et al., 1999). Alternatively, the inhibition of splicing by disrupting the intron-5′UTR base pairing may be a consequence of the relief of the translational stall: since the 5′ splice site is contained within the 3′ end of the *HAC1*^{u} ORF, the passage of translating ribosomes might prevent the 5′ splice site from assuming a suitable secondary structure and thus prevent cleavage. Indeed, in the mutants with disrupted base pairing, significant amounts of a smaller form of *HAC1* mRNA accumulated upon UPR induction (marked with one asterisk in Figure 3B). Based on its size and hybridization with a 5′ exon-specific probe, this band is likely to correspond to the 5′ exon-intron splicing intermediate (Cox and Walter, 1996; Sidrauski et al., 1996), indicating that cleavage at the 5′ splice site is impaired in the base pair-disrupted *HAC1*^{u} mRNA mutants. In agreement with this interpretation, splicing was more severely impaired in the mutant that was more efficiently translated (Figures 3B and 3C, compare pJL179 and pJL178). Attenuation of translation may therefore be essential to keep *HAC1*^{u} mRNA in a fully splicing-competent state.

Intriguingly, splicing can occur on *HAC1*^{u} mRNA associated with stalled ribosomes. The notion that polyribosome-associated *HAC1*^{u} mRNA is a splicing substrate further underscores the view that splicing is a cytoplasmic event. The disposition of Ire1p as an integral ER-membrane protein with its nuclease domain facing the cytoplasm is consistent with a cytoplasmic mecha-

nism. tRNA ligase has been localized to the nucleus but, upon overexpression, was also detectable in the cytoplasm (Clark and Abelson, 1987). It is therefore likely that a sufficient amount of tRNA ligase is constitutively located in the cytoplasm or that tRNA ligase shuttles between the two compartments. Cytoplasmic splicing of polyribosome-associated *HAC1*^{u} mRNA thus is a plausible mechanism, although we cannot rule out that nuclear splicing of newly transcribed mRNA can also occur. Ribosomes that are preinitiated and stalled on *HAC1*^{u} mRNA could finish translation after the intron is removed, thus leading to a rapid initial burst of Hac1p^i synthesis, perhaps to provide cells with an exceedingly rapid response to changing needs in the ER.

Experimental Procedures

Plasmids
GFP Constructs
All parts of the following constructs were generated by PCR amplification, sequenced, and assembled between the PstI and ApaI sites of pRS315. Expression is driven by the GPD promoter (nt −676 to −37 of *TDH3* flanked by a PstI site at the 5′ and a SmaI site at the 3′ end; +1 refers in all constructs to the first nucleotide of the start codon of the corresponding gene). The 5′UTR is either from *HAC1* (nt −67 to −1; nt −67 corresponds to the 5′ end of both *HAC1*^{u} and *HAC1*^{i} mRNA as mapped by primer extension and S1 analysis) or from the *Xenopus* β-globin gene (as present in pSPUTK) and flanked by SmaI and XbaI sites at the 5′ and 3′ end, respectively. The ORF of GFP is cloned downstream of the XbaI site and is followed by the *ACT1* 3′UTR (the *ACT1* stop codon plus 381 nt). In some constructs, the *HAC1* intron (flanked by 37 nt of the 5′ and 29 nt of the 3′ exon) is inserted between the stop codon of GFP and the *ACT1* 3′UTR.

HAC1 Constructs for In Vitro Transcription/Translation
All inserts were cloned 3′ of the SP6 promoter and 5′ of the KpnI site of pSPUTK and carry a poly(A) tail at the 3′ end. The poly(A) tail is flanked by a NotI site at the 5′ end and an XbaI site at the 3′ end, which allows the production of transcripts without or with poly(A) tail. The *HAC1* sequences are based on pJC316 (Cox and Walter, 1996). The anticipated sequences of the inserts were confirmed by sequencing. pUR10 (hac·HAC·hac; used for the experiment in Figure 2) contains the first 5 nt of the pSPUTK 5′ leader sequence followed by nt −75 to +1273 of HA-*HAC1*. pUR6 (hac·HAC·hac; used for the experiment in Figure 2C) is as pUR10 but contains nt −75 to +1397 of HA-*HAC1*. pUR11 (glo·HAC·hac) contains the entire 5′ leader sequence of pSPUTK followed by nt +1 to +1273 of HA-*HAC1*. pUR9 (hac·HAC·act) is as pUR10 up to the Hac1p^u stop codon, which is followed by a linker of 32 nt and the *ACT1* 3′UTR as described for the GFP constructs. pUR8 (glo·HA-C·act) is as pUR11 up to the Hac1p^u stop codon, which is followed by a linker of 32 nt and the *ACT1* 3′UTR as described for the GFP constructs.

HAC1 5′UTR-Intron Interaction Mutants
Mutations were introduced into pJC316 with the QuikChange site-directed mutagenesis kit (Stratagene) and confirmed by sequencing. The following three plasmids are identical with pJC316 except for the regions indicated: pJL178: nt −38 to −22 of HA-*HAC1* were replaced with 5′ TTGGCCGAGGAGGGGGT 3′; pJL179: nt +796 to +815 of HA-*HAC1* were replaced with 5′ ACCCCCTCCTCCT CCAAAA 3′; pJL177 carries the mutations of both pJL178 and pJL179.

2′-O-Methyl Oligoribonucleotides
2′-O-methyl oligoribonucleotides with the following sequences were used in in vitro translation experiments: 5′ UCUCUUGACGAGUA CAGGGAU 3′ (sense-ORF), 5′ GGUGGGGGAGGAGGAGGUU 3′ (anti-5′UTR), 5′ AACCGGCUCCUCCCCCAUC 3′ (antiintron).

Isolation of Total RNA and Northern Blot Analysis
Total RNA for Northern blot analysis was isolated from yeast cells with a scaled-down and simplified version of the hot-phenol extrac-

tion procedure described by Köhrer and Domdey (1991). Northern blot analysis was carried out as described (Cox and Walter, 1996), but blots were washed in 2× SSC with 0.1% w/v SDS and quantitated on a Storm 840 imaging system with the ImageQuant software v1.2 (Molecular Dynamics). The amount of splicing was defined as the ratio of $HAC1^i$ and the sum of $HAC1^u$ and $HAC1^i$ multiplied by 100 (% splicing).

All probes were generated by PCR amplification and were labeled with [α-^{32}P]dCTP and Ready-To-Go DNA labeling beads (Pharmacia Biotech). The GFP probe was directed against the coding region of GFP, the *SCR1* probe against the full-length *SCR1* RNA, the *HAC1*-5′ exon/intron probe against nt −45 to +986 of *HAC1*, and the *HAC1*-5′ exon probe against nt −45 to +626 or nt +375 to +653 of *HAC1*.

Isolation of Proteins from Yeast Cells
Cells were collected from cultures by filtration, frozen in liquid nitrogen and disrupted in ∼500 μl 8 M urea by vortexing for 5 min at 4°C in the presence of 500 μl 0.5 mm Zir/Silica beads. After adding 75 μl 20% w/v SDS, the samples were boiled for 5 min and the lysates cleared by centrifugation at 20,800 × g for 5 min at room temperature. The protein concentrations of the lysates were determined with the BCA protein assay from Pierce.

Analysis of GFP-Expressing Strains
Analysis on Plates
The yeast strain W303 (*MAT A, ade2-1, trp1-1, can1-100, leu2-3, -112, his3-11, -15, ura3*) was transformed with pRS315 carrying no insert or one of the four GFP constructs, plated on selective minimal medium without leucine and the plate scanned with the fluorescent scanner FluorImager SI (emission filter 530 DF 30; Molecular Dynamics).
Analysis in Liquid
The same strains as analyzed on a plate were grown in selective minimal medium without leucine to optical densities at 600 nm (OD_{600}) of 0.3 to 0.7. The cultures were sonicated immediately prior to analysis and the fluorescence of the cells measured with a Becton Dickinson FACScan flow cytometer. The mean fluorescence of uniform cell populations was determined with the software CellQuest v3.3. The amount of mRNA encoding GFP relative to the amount of *SCR1* RNA was determined from aliquots of the same cultures by Northern blot analysis.

In Vitro Transcription
Plasmids pUR6, pUR8, pUR9, pUR10, and pUR11 were linearized with NotI and used as templates in in vitro transcription reactions. Capped RNA transcripts were prepared with SP6 RNA polymerase in the presence of m^{7}G(5′)ppp(5′)G according to standard procedures. Note that transcription from NotI-linearized pUR6 terminates prematurely leading to a uniform population of transcripts of ∼1400 nt. The transcripts were purified by extracting with phenol/chloroform and subsequent ethanol precipitation and resuspended in water. The RNA concentrations were calculated based on the absorbance at 260 nm and the relative amounts and the integrity of the transcripts were verified by Northern blot analysis.

In Vitro Translation
Yeast extracts for in vitro translation experiments were prepared from strain yAS1874 (*MATa, ade2, his3, leu2, trp1, ura3, mak10::URA3, pep4::HIS3, Δprb1, Δprc1*; a kind gift from Dr. Alan Sachs) according to Tarun and Sachs (1995) with the following modifications: cells from 1 liter of an OD_{600} = 1.5 yeast culture in YPD were harvested by centrifugation at 4°C and washed four times. Buffer A contained 30 mM HEPES-KOH (pH 7.4), 100 mM KOAc, 2 mM Mg(OAc)₂, 0.5 mM DTT, 0.5 mM phenylmethylsulfonyl fluoride (PMSF), 0.4 μg/ml leupeptin hemisulfate, and no mannitol throughout the whole procedure.

Fifteen microliter in vitro translation reactions were set up as described by Tarun and Sachs (1995) with nuclease-treated extract and 200 fmol-capped RNA and 3.6 to 5 μCi L-[^{35}S]methionine instead of unlabeled methionine. The samples were incubated at room temperature (26°C) and the reactions stopped at the time indicated by mixing with equal volumes of 2× SDS-protein gel sample buffer. Five to fifteen microliter aliquots of the stopped reactions were

separated by electrophoresis through 10%–15% SDS-polyacrylamide gels. Gels were stained with Coomassie blue, destained, dried, and the amount of full-length HA-Hac1p^u (all forms) determined by quantitation on a Storm 840 imaging system with the ImageQuant software v1.2 (Molecular Dynamics).

Where indicated, 2 or 20 pmol 2′-O-methyl oligoribonucleotide were annealed to 200 fmol hac·HAC·hac or hac·HAC·act in 20 mM HEPES-KOH (pH 7.4)/100 mM KOAc by heating to 95°C for 90 s and then cooling down to room temperature over 40 min.

Analysis of *HAC1* Polyribosomes
pJC316, pJL177, pJL178, and pJL179 were transformed into yJL118 (W303 except *hac1::URA3*) and the resulting strains grown in 400 ml synthetic medium without histidine but supplemented with 100 μg/ml myo-inositol. At OD_{600} ≅ 0.7, 600 μl 1 M DTT were added to 75 ml aliquots of the cultures to induce *HAC1* splicing. After 50 min at 30°C, aliquots from the treated and untreated cultures were taken for RNA and protein analysis.

To isolate polyribosomes, 1 ml 15 mg/ml cycloheximide was added to 250 ml of the same cultures as used for the RNA and protein preparations, but at OD_{600} ≅ 1.3. After 10 min at 30°C, cells were harvested by centrifugation at room temperature. All subsequent steps were carried out at 0–4°C with ice-cold buffer. Cells were washed twice with 50 ml LBC (30 mM HEPES-KOH [pH 7.4], 100 mM KOAc, 30 mM Mg(OAc)₂, 0.5 mM DTT, 0.5 mM PMSF, 0.4 μg/ml leupeptin hemisulfate), resuspended in LBC (1 ml final volume) and sodium heparin was added to 0.2 mg/ml. Cells were disrupted by vortexing in the presence of 500 μl 0.5 mm Zir/Silica beads. The lysates were cleared by centrifugation at 5,200 × g, then at 10,600 × g, and finally at 20,800 × g for 5 min each. Aliquots (10 OD$_{260}$) of each extract were layered on top of 13 ml 10%–50% w/v sucrose gradients in GBL (30 mM HEPES-KOH [pH 7.4], 50 mM KOAc, 12 mM Mg(OAc)₂, and 0.1 mg/ml sodium heparin) and spun in a SW 40 Ti rotor (Beckman) at 40000 rpm (285,000 × g$_{max}$) for 100 min at 4°C. Fractions of the gradients (750 μl for Figures 4A and 4B, 180 μl for Figure 4C, or 500 μl for Figure 5B) were collected with a density gradient fractionator from ISCO (model 185) while recording the absorbance profile at 254 nm. RNA was isolated by phenol/chloroform extraction followed by precipitation with isopropanol or ethanol. Five percent of the loads and fifty percent of each fraction were analyzed by Northern blot.

Preparation of extracts and fractionation from KRY80 cells (*sec12-1, MATα, trp1-289, leu2, his4, ura3-52*) was identical but sucrose gradients contained 100 mM KOAc and 30 mM Mg(OAc)₂.

Transcription Shut-off
The yeast strain JC218 (Sidrauski et al., 1996; *rpb1-1*) was grown in 260 ml YPD at room temperature to OD_{600} ≅ 0.5 and the cells were pelleted by centrifugation. The cells were resuspended in 260 ml YPD (pH 5.4), which was prewarmed to 37°C, and the culture split into three 60 ml aliquots. The UPR was induced by adding 480 μl 1 M DTT to each 60 ml aliquot after 10, 20, and 40 min, respectively at 37°C. Ten milliliter aliquots were taken of each culture immediately before and 5, 10, 20, and 40 min after the addition of DTT. Cells were harvested by centrifugation and frozen in liquid nitrogen.

References

Bertolotti, A., Zhang, Y., Hendershot, L.M., Harding, H.P., and Ron, D. (2000). Dynamic interaction of BiP and ER stress transducers in the unfolded-protein response. Nat. Cell Biol. *2*, 326–332.

Chapman, R.E., and Walter, P. (1997). Translational attenuation mediated by an mRNA intron. Curr. Biol. *7*, 850–859.

Clark, M.W., and Abelson, J. (1987). The subnuclear localization of tRNA ligase in yeast. J. Cell Biol. *105*, 1515–1526.

Clark, I.E., Wyckoff, D., and Gavis, E.R. (2000). Synthesis of the posterior determinant Nanos is spatially restricted by a novel co-translational regulatory mechanism. Curr. Biol. *10*, 1311–1314.

Cox, J.S., and Walter, P. (1996). A novel mechanism for regulating activity of a transcription factor that controls the unfolded protein response. Cell *87*, 391–404.

Cox, J.S., Shamu, C.E., and Walter, P. (1993). Transcriptional induction of genes encoding endoplasmic reticulum resident proteins requires a transmembrane protein kinase. Cell *73*, 1197–1206.

Gonzalez, T.N., Sidrauski, C., Dörfler, S., and Walter, P. (1999). Mechanism of non-spliceosomal mRNA splicing in the unfolded protein response pathway. EMBO J. *18*, 3119–3132.

Gray, N.K., and Wickens, M. (1998). Control of translation initiation in animals. Annu. Rev. Cell Dev. Biol. *14*, 399–458.

Johansson, H.E., Belsham, G.J., Sproat, B.S., and Hentze, M.W. (1994). Target-specific arrest of mRNA translation by antisense 2′-O-alkyloligoribonucleotides. Nucleic Acids Res. *22*, 4591–4598.

Kaufman, R.J. (1999). Stress signaling from the lumen of the endoplasmic reticulum: coordination of gene transcriptional and translational controls. Genes Dev. *13*, 1211–1233.

Kawahara, T., Yanagi, H., Yura, T., and Mori, K. (1997). Endoplasmic reticulum stress-induced mRNA splicing permits synthesis of transcription factor Hac1p/Ern4p that activates the unfolded protein response. Mol. Biol. Cell *8*, 1845–1862.

Köhrer, K., and Domdey, H. (1991). Preparation of high molecular weight RNA. Methods Enzymol. *194*, 398–405.

Kozak, M. (1989). Circumstances and mechanisms of inhibition of translation by secondary structure in eucaryotic mRNAs. Mol. Cell. Biol. *9*, 5134–5142.

Lee, R.C., Feinbaum, R.L., and Ambros, V. (1993). The *C. elegans* heterochronic gene *lin-4* encodes small RNAs with antisense complementarity to *lin-14*. Cell *75*, 843–854.

Mehlin, H., Daneholt, B., and Skoglund, U. (1992). Translocation of a specific premessenger ribonucleoprotein particle through the nuclear pore studied with electron microscope tomography. Cell *69*, 605–613.

Mori, K. (2000). Tripartite management of unfolded proteins in the endoplasmic reticulum. Cell *101*, 451–454.

Mori, K., Ma, W., Gething, M.-J., and Sambrook, J. (1993). A transmembrane protein with a cdc2$^+$/CDC28-related kinase activity is required for signaling from the ER to the nucleus. Cell *74*, 743–756.

Nonet, M., Scafe, C., Sexton, J., and Young, R. (1987). Eucaryotic RNA polymerase conditional mutant that rapidly ceases mRNA synthesis. Mol. Cell. Biol. *7*, 1602–1611.

Novick, P., Field, C., and Schekman, R. (1980). Identification of 23 complementation groups required for post-translational events in the yeast scretory pathway. Cell *21*, 205–215.

Oka, T., Nishikawa, S., and Nakano, A. (1991). Inhibition of GTP hydrolysis by Sar1p causes accumulation of vesicles that are a functional intermediate of the ER-to-Golgi transport in yeast. J. Cell Biol. *114*, 671–679.

Olsen, P.H., and Ambros, V. (1999). The *lin-4* regulatory RNA controls developmental timing in *Caenorhabditis elegans* by blocking LIN-14 protein synthesis after the initiation of translation. Dev. Biol. *216*, 671–680.

Patil, C., and Walter, P. (2001). Intracellular signaling from the endoplasmic reticulum to the nucleus: the unfolded protein response in yeast and mammals. Curr. Opin. Cell Biol. *13*, 349–355.

Shamu, C.E., and Walter, P. (1996). Oligomerization and phosphorylation of the Ire1p kinase during intracellular signaling from the endoplasmic reticulum to the nucleus. EMBO J. *15*, 3028–3039.

Sidrauski, C., and Walter, P. (1997). The transmembrane kinase Ire1p is a site-specific endonuclease that initiates mRNA splicing in the unfolded protein response. Cell *90*, 1031–1039.

Sidrauski, C., Cox, J.S., and Walter, P. (1996). tRNA ligase is required for regulated mRNA splicing in the unfolded protein response. Cell *87*, 405–413.

Spena, A., Krause, E., and Dobberstein, B. (1985). Translation efficiency of zein mRNA is reduced by hybrid formation between the 5′- and 3′-untranslated region. EMBO J. *4*, 2153–2158.

Tarun, S.Z., Jr., and Sachs, A.B. (1995). A common function for mRNA 5′ and 3′ ends in translation initiation in yeast. Genes Dev. *9*, 2997–3007.

Travers, K.J., Patil, C.K., Wodicka, L., Lockhart, D.J., Weissman, J.S., and Walter, P. (2000). Functional and genomic analyses reveal an essential coordination between the unfolded protein response and ER-associated degradation. Cell *101*, 249–258.

Urano, F., Bertolotti, A., and Ron, D. (2000). IRE1 and efferent signaling from the endoplasmic reticulum. J. Cell Sci. *113*, 3697–3702.

van den Heuvel, J.J., Planta, R.J., and Raue, H.A. (1990). Effect of leader primary structure on the translational efficiency of phosphoglycerate kinase mRNA in yeast. Yeast *6*, 473–482.

Vega Laso, M.R., Zhu, D., Sagliocco, F., Brown, A.J., Tuite, M.F., and McCarthy, J.E. (1993). Inhibition of translational initiation in the yeast *Saccharomyces cerevisiae* as a function of the stability and position of hairpin structures in the mRNA leader. J. Biol. Chem. *268*, 6453–6462.

Welihinda, A.A., and Kaufman, R.J. (1996). The unfolded protein response pathway in *Saccharomyces cerevisiae*. Oligomerization and trans-phosphorylation of Ire1p (Ern1p) are required for kinase activation. J. Biol. Chem. *271*, 18181–18187.

Wightman, B., Ha, I., and Ruvkun, G. (1993). Posttranscriptional regulation of the heterochronic gene *lin-14* by *lin-4* mediates temporal pattern formation in *C. elegans*. Cell *75*, 855–862.